Force Field for Computation of Conformational Energies, Structures, and Vibrational Frequencies of Aromatic Polyesters

H. SUN

Biosym Technologies, Inc., 9685 Scranton Road, San Diego, California 92121

Received 6 October 1993; accepted 6 January 1994

ABSTRACT

A CFF93[1] all-atom force field for aromatic polyesters based on *ab initio* calculations is reported. The force field parameters are derived by fitting to quantum mechanical data which include total energies, first and second derivatives of the total energies, and electrostatic potentials. The valence parameters and the *ab initio* electrostatic potential (ESP) derived charges are then scaled to correct the systematic errors originating from the truncation of the basis functions and the neglect of electron correlation in the HF/6-31G* calculations. Based on the force field, molecular mechanics calculations are performed for homologues of poly(*p*-hydroxybenzoic acid) (PHBA) and poly(ethylene terephthalate) (PET). The force field results are compared with available experimental data and the *ab initio* results. © 1994 by John Wiley & Sons, Inc.

Introduction

Computer simulation of the properties of high polymers has become an active research subject in recent years,[2-4] partly because of the rapid progress in modern computer architecture which offers the possibility of performing quantitative, atomistic molecular dynamics (MD), or Monte Carlo (MC) simulations for large molecular systems. An underlying issue of all atomistic simulations is the quality of the force field, which consists of a set of analytical function forms and parameters and provides a detailed description of inter- and intramolecular interactions as functions of molecular structures and relative positions. The accuracy of the force field directly influences the reliability of the simulations. Because of this, there has been a growing interest in force field development.[1,5-22] This article reports an all-atom force field for computer simulations of aromatic polyesters. In particular, the force field is developed for poly(*p*-hydroxybenzoic acid (PHBA) and

Journal of Computational Chemistry, Vol. 15, No. 7, 752–768 (1994)

CCC 0192-8651/94/070752-17

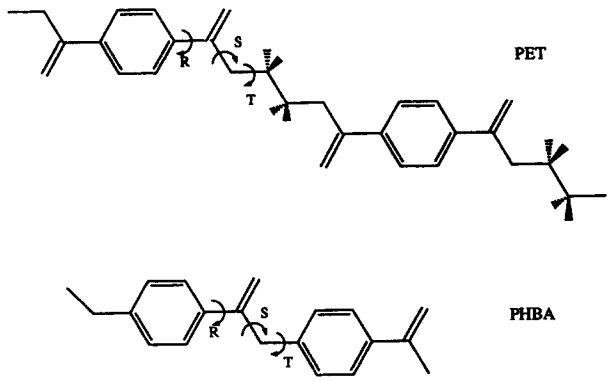

FIGURE 1. Illustration of two aromatic polyesters, poly(*p*-hydroxybenzoic acid) (PHBA) and poly(ethylene terephthalate) (PET). Conformations of internal rotations about bonds *R*, *S*, and *T* are particularly interesting in this and other studies.

poly(ethylene terephthalate) (PET), as illustrated in Figure 1.

As a group of both academically and industrially important materials, aromatic polyesters have been studied by many authors using different theoretical methods. Many of these efforts to characterize conformational structures and energies have been based on *ab initio*, semiempirical, and force field computations on small analogues of the polymers. One of the earliest efforts was reported by Hehre et al.,[23] who conducted Hartree–Fock calculations with the STO-3G basis set[24] for a group of monosubstituted benzenes. Schaeffer et al.[25,26] calculated structures and internal rotational barriers of phenol and a number of benzoyl derivatives at the same level of theory. Calculations with split-valence basis sets—3-21G[27] and 4-21G[28]—were reported by Marriott et al.,[29] who demonstrated that the calculated energy barriers for rotation about C(phenyl)—X bonds are less satisfactory with the split valence basis sets than with the minimum basis set. Specifically, with the STO-3G basis functions, Hartree–Fock calculations predicted that the barrier height for rotation about the C(carbonyl)—C(phenyl) bond (R bond in Fig. 1) in methyl benzoate is 5.05 kcal/mol,[26,29] which agrees well with the experimental value of 5.30 kcal/mol.[30] However, larger basis sets, 3-21G and 4-21G, led to worse results.[29] Recently, Coussens et al.[31] systematically studied the effects of basis sets and electron correlation by calculating the energy barrier heights of rotation about the R bond in benzaldehyde. They concluded that "in order to obtain satisfactory agreement with experimental data, the required level of sophistication of the *ab initio* calculations becomes intractable for practical modeling purpose."[31] The difficulty of calculating conformational energies using *ab initio* techniques has been well recognized,[32,33] and it is generally true that very large basis sets and high-level corrections for electron correlation are required to calculate the rotational energies accurately.[33] In addition to the *ab initio* calculations, semiempirical calculations, such as AM1 and MNDO, have been reported in the literature.[31,34–36] By comparing the calculated rotational barriers with experimental results[30,37,38] for a group of conjugated molecules, Fabian[34] reported that the AM1 results are 50% too low. Later, this conclusion was supported by Coussens et al.[31] Unlike the *ab initio* calculations, there is no systematical way to improve the accuracy of calculations for semiempirical calculations.

Because of the difficulties faced by the *ab initio* and semiempirical calculations, force field methods become more attractive. The basic assumptions of the force field method include the transferability of molecular interactions between similar molecular environments and the additivity of energy contributions (i.e., the total energy of a large molecule is simply an addition of all contributions from the smaller segments of which the molecule consists). Using these assumptions, a force field can be developed for small molecules for which highly accurate experimental and theoretical studies may be carried out and many data are already available in the literature. The results can then be transferred to larger molecules, including polymers.

The first molecular mechanics force field developed for aromatic polyesters is perhaps that presented by Hummel and Flory,[39] based on then available crystal structural data and conformational energies of rotation about the C(phenyl)—C(carbonyl) bond. The functional forms that these authors used are harmonic terms for both bond stretching and bending, Hill's 6-exp function[40] for nonbonded interactions, and a so-called electron delocalization energy term for bond torsion: $E = -B\cos^2\phi$. Electrostatic terms were omitted. The reference bond lengths and angles were taken from X-ray crystal data, and the force constants were taken from the report of Allinger and Chang.[41] The *B* parameters were made consistent with experimental results. Later, Coulter and Windle[35] parameterized an MM2[9] type of force field for the aromatic esters. They modified the MM2 parameters based on the semiempirical AM1 calculations and a survey of available crystal and other experimental data. The MM2 force field uses harmonic potential

for bond stretching and bending, the same as that of Hummel and Flory's force field. For torsions, a three-parameter Fourier expansion was used.

The present force field is a CFF93[1] type force field which is different from the earlier developed force fields, such as MM2,[9] CVFF,[11] etc. First, the present force field uses much more complex functional forms. Anharmonic terms are used for bonds and angles, Fourier expansion is employed for torsions, extensive cross-coupling terms are included, and the nonbonded interactions are written explicitly in terms of both van der Waals forces and electrostatic interactions. Consequently, the present force field is much more flexible and potentially able to predict not only equilibrium geometries and conformational energies, but also more difficult properties such as conformation-related structure changes, electrostatic potentials, and vibrational frequencies. Second, the method used to derive the force field in this study is based on both *ab initio* calculations and experimental data fitting, whereas most other force fields[7-17,35,39] are parameterized mainly from experimental data. Because the quantum mechanical *ab initio* calculations can provide a great amount of information with reasonable accuracy, the parameterization of a very complex force field becomes much easier than with the traditional approach.

Method, Functional Forms, and Parameters

All calculations reported in this article were conducted on an IBM RISC/6000 550 workstation. The *ab initio* software packages TURBOMOLE[42] and GAUSSIAN90[43] with direct self-consistent field (SCF) method were used. Geometry optimizations were conducted by using the gradient minimization algorithm provided by these software packages. The total energies, analytic gradients, and Hessians matrixes were calculated. The calculations of *ab initio* electrostatic potentials (ESP) and the fit of partial charges to the ESP were performed by using TURBOMOLE. The valence and cross-coupling parameters were fitted by using PROBE.[44] All molecular mechanics calculations were conducted by using DISCOVER.[44]

A two-step procedure was used to parameterize this force field. First, a quantum mechanical force field was developed by least squares fitting to the *ab initio* data, which includes electrostatic potentials, energies, and first and second derivatives of the energies. Then the quantum mechanical force field was scaled by a set of generic parameters[1,5] to correct the systematic errors of the *ab initio* calculations to produce the final force field. The parameterization procedure[1] starts by selecting a group of model compounds which resemble the molecular systems of interest. Figure 2 lists the model compounds selected for this study: benzaldehyde, benzoic acid, methyl benzoate, ethyl benzoate, phenyl benzoate, and terephthalic acid. The most relevant molecules to PET and PHBA, among these model compounds, are ethyl benzoate, phenyl benzoate, and terephthalic acid. Smaller molecules were included to represent short-distance interactions (bonds and angles) to reduce the amount of computation. For the convenience of discussion, all heavy atoms and hydroxyl hydrogen atoms (Fig. 2) are labeled by numbers. Alkyl and phenyl hydrogen atoms are not labeled explicitly, and they will be referred to by the carbon atoms that they are attached to, such as $H(C_5)$, $H(C_6)$, etc.

For these model compounds, *ab initio* calculations were performed to optimize the structures. To be consistent with our research program and to transfer already derived parameters directly, Hartree–Fock calculations with the 6-31G* basis functions[45] were conducted. Following common nomenclature, these calculations are referred to as HF/6-31G* in this article. The optimized geometries include not only global minima but also those local minima and transition states which are crucial for describing the conformational energy surfaces. From those optimized structures, the potential surfaces were further sampled by randomly distorting each of the optimized structures along their normal mode coordinates. The extent of the sampling was controlled by setting a cutoff energy to avoid very high energy structures and by varying the number of distorted structures to ensure that a good representation of each internal degree of freedom was obtained. For each of the optimized and distorted structures, *ab initio* total energies and first and second derivatives of the energies (gradients and Hessians) were calculated. All of these quantities were used to least squares fit the potential function:

$$E_{\text{total}} = \Sigma E^{(b)} + \Sigma E^{(a)} + \Sigma E^{(t)} + \Sigma E^{(o)} + \Sigma E^{(bb')} + \Sigma E^{(ba)} + \Sigma E^{(bt)} + \Sigma E^{\text{vdw}} + \Sigma E^{\text{elec}} \quad (1)$$

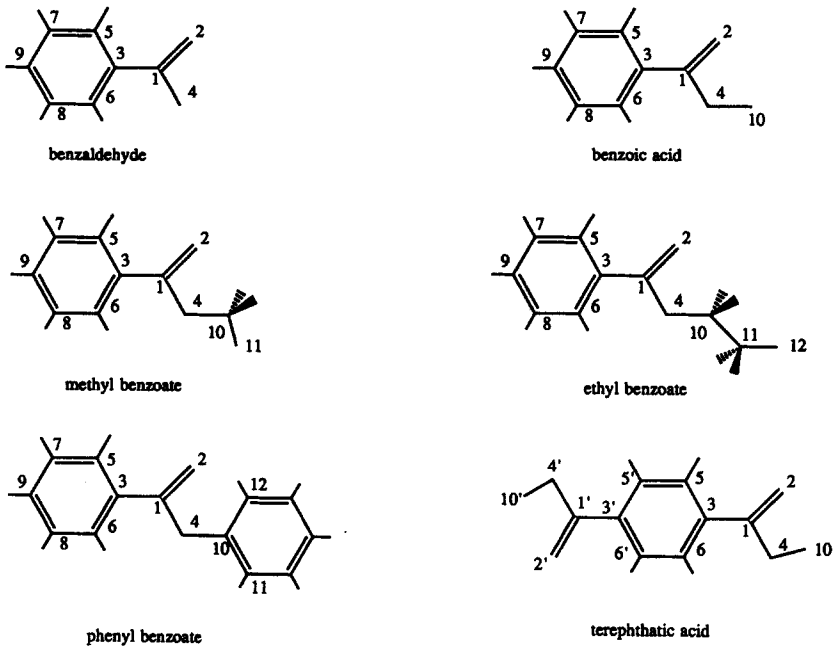

FIGURE 2. Illustration of the model compounds which are used to sample the molecular interactions of aromatic polyesters.

where

$$E^{(b)} = \sum_{n=2}^{4} k_n^{(b)} (b - b_o)^n$$

$$E^{(a)} = \sum_{n=2}^{4} k_n^{(a)} (\theta - \theta_o)^n$$

$$E^{(t)} = \sum_{n=1}^{3} k_n^{(t)} (1 - \cos n\phi)$$

$$E^{(o)} = k^{(o)} (\chi - \chi_o)^2 \qquad (2)$$

$$E^{(bb')} = k^{(bb')} (b - b_o)(b' - b_o')$$

$$E^{(ba)} = k^{(ba)} (b - b_o)(\theta - \theta_o)$$

$$E^{(bt)} = (b - b_o) \sum_{n=1}^{3} k_n^{(bt)} \cos n\phi \qquad (3)$$

and

$$E^{\text{vdw}} = \varepsilon[2(r^*/r)^9 - 3(r^*/r)^6]$$

$$E^{\text{elec}} = \frac{Q_i Q_j}{r_{ij}} \qquad (4)$$

The total energy is divided into three major categories: (1) contributions from each of the internal valence coordinates, (2) cross-coupling terms between internal coordinates, and (3) nonbonded interactions. The valence energies consist of terms from distortions of bond lengths E^b, bond angles E^a, out-of-plane bending angles E^o, and torsion angles E^t. Both bond and angle terms contain anharmonic constants to quartic terms to characterize anharmonic features. The torsion function is represented by a symmetric Fourier expansion. The out-of-plane function is considered to be a simple harmonic function. To minimize the number of parameters without sacrificing the accuracy substantially, only three cross-coupling terms are used in this force field: $E^{bb'}$ is the interaction between two bonds with one common atom, E^{ab} represents the coupling between a bond and an angle in which the bond is one of the edges, and E^{bt} stands for interactions between a bond and a dihedral angle of rotation about the bond. The nonbonded energies include intramolecular nonbonded interactions, which are interactions between any pair of atoms that belong to same molecule but are separated by at least two intervening atoms, and intermolecular nonbonded interactions, which are the interactions between any pair of atoms that belong to different molecules. The nonbonded energies are subsequently divided into van der Waals interactions E^{vdw} and electrostatic interactions E^{elec}. A 6–9 Lennard–Jones function[46] is used to represent the van der Waals forces, whereas the electrostatic interaction is written in the form of a standard Coulombic interaction with partial atomic

charges. To obtain transferable parameters, charges are further written as a sum of bond increments δ_{ij}, which are defined as a charge displacement from atom i to atom j. For each atom i, the charge is a sum δ_{ij}, where j runs over all atoms that are directly bonded to atom i,

$$Q_i = \sum_j \delta_{ij} \tag{5}$$

Because of the definition, the bond increment for any pair of like atoms is zero.

Atom types are used to define the interactions in the force field. An atom type represents a group of chemically equivalent atoms which share the same van der Waals parameters and some other force field parameters. For example, in the CFF93 force field,[1,5] alkyl carbons are designated as atom type c, phenyl atoms are assigned as atom type cp, and both alkyl and phenyl hydrogen atoms are represented by atom type h. These three atom types are used in this force field, and the related parameters are transferred from the CFF93 force field.[5] In Table I, the atom types defined to describe the force field for polyesters are given. In addition to the c, cp, and h atom types, four new atom types are given, namely c_1, o_1, o_2, and ho2, to designate carbonyl carbons, oxygens, ester oxygens, and hydroxyl hydrogens, respectively. The van der Waals parameters of these atom types are also given in this table. These parameters were derived independently by fitting crystal structures of a group of compounds with similar functional groups.[6,47] Direct comparison of these van der Waals parameters with those reported in the literature is difficult because the functional forms may be different. For example, rather large well depths ε and small van der Waals diameters r^* are obtained for ho2, o_1, and o_2 because these atoms may be involved in hydrogen bonds, but the present force field does not use a special functional form for hydrogen bonds.

The electrostatic parameters, or bond increments, of the aromatic ester group were derived from *ab initio* calculations. Several methods have been proposed and used in the literature[48–56] to derive atomic partial charges from *ab initio* calculations. The most popular and widely used method is perhaps the Mulliken population analysis (MPA).[48,49] However, it is well known that the MPA charges are dependent on the basis functions used in the *ab initio* calculations. The atomic polar tensor method[50] has been proposed for planar molecular systems. Dinur and Hagler[50] showed that for such a molecule, the atomic partial charges used to calculate electrostatic energies can be defined by the Cartesian out-of-plane derivatives of the molecular dipole moment. It was shown that these charges reproduce the molecular dipole moment exactly for a planar system. Consequently, these charges can represent most features of the electrostatic potential energy surface for a polar molecule, of which the molecular dipole moment dominates the electrostatic interactions. The limitation of this approach is apparently that it works only for planar systems. Much progress has been made recent years in least squares fitting of the electrostatic potentials (ESP) to derive charges or multipoles for a molecule.[51–56] In this approach, the electrostatic potential is represented by values on a set of grid points around the molecule. The atomic charges or multipoles are then treated as parameters to fit the electrostatic potentials. Although the fitted results are generally related to the way that the grid points are placed,[51–54] this influence can be minimized by increasing the number of grid points[53] and arranging the grid points properly.[51–53] The calculated charges are far less sensitive to the basis sets than are the MPA charges. More importantly, the physical meaning of the charges obtained from the ESP

TABLE I.
Atom Types and van der Waals Parameters for the Force Field of Aromatic Polyester.

Atom type	r^*	ε	Description	Relevant atoms
c_1	3.308	0.120	Carbonyl carbon	C_1
o_1	3.200	0.257	Carbonyl oxygen	O_2
o_2	3.320	0.240	Ester oxygen	O_4
ho2	1.110	0.015	Hydroxy hydrogen	H_{10}
c	4.010	0.054	Alkyl carbon	C_{10}, C_{11}
cp	4.010	0.064	Phenyl carbon	C_3, C_4, C_5, C_6, C_7, C_8, C_9
h	2.995	0.020	Alkyl and phenyl	$H(C_3–C_9)$, $H(C_{10}–C_{11})$

fitting is clear—they reproduce the electrostatic potential surfaces in a least squares sense. Based on these considerations, the ESP method was used in this study to derive atomic partial charges.

A spherical grid model in which the grid points were placed symmetrically on several concentric spherical shells around each of the nuclei was used in this study. The first shell was placed at a distance 1 Å greater than the "standard" van der Waals radii (1.7 Å for C, 1.4 Å for O, and 1.2 Å for H) from each of the nuclei in the molecule. Ten more shells of grids were placed at the distances of 2, 3, 4, 5, 6, 7, 8, 10, 12, and 16 Å greater than the van der Waals radii. A total of 4000 points were placed on each of the shells. However, in the region where two or more spheres overlap, some grid points were removed from the region to avoid oversampling.

Figure 3 presents the calculated partial charges for benzoic acid and methyl, ethyl, and phenyl benzoates. All were calculated for the HF/6-31G* optimized structures, using the grid points as described earlier. The least squares fits were generally satisfactory, with the root of mean square (RMS) deviations below 0.26 kcal/mol.

Examination of the atomic charges given in Figure 3 reveals that the chemical structures have considerable influence on the charges calculated. It has been shown[6,53–56] that the ESP charges are also dependent on the conformations. These dependencies reflect the weakness of the point charge model rather than the method itself. It is well known[51–59] today that the point charge model is insufficient to represent accurately the electrostatic potential surfaces.

However, the atomic point charge model has its advantages: It provides a simple, fast approach to calculating the electrostatic interactions, and the efficiency of energy computation is still one of the most important factors for simulations of large molecular systems. Although the model is not highly accurate, it can describe qualitatively the most important features of the electrostatic potentials as a first-order approximation, as we will demonstrate later in this section. Based on this consideration, the point charge model is used for the present force field.

The average charge parameters for the model compounds were derived as follows. Because the bond increments for alkyl and phenyl groups were transferred,[5] there are only four new bond increments that need to be parameterized. To obtain these parameters, all atomic charges of the alkyl or phenyl group were summed and the net total

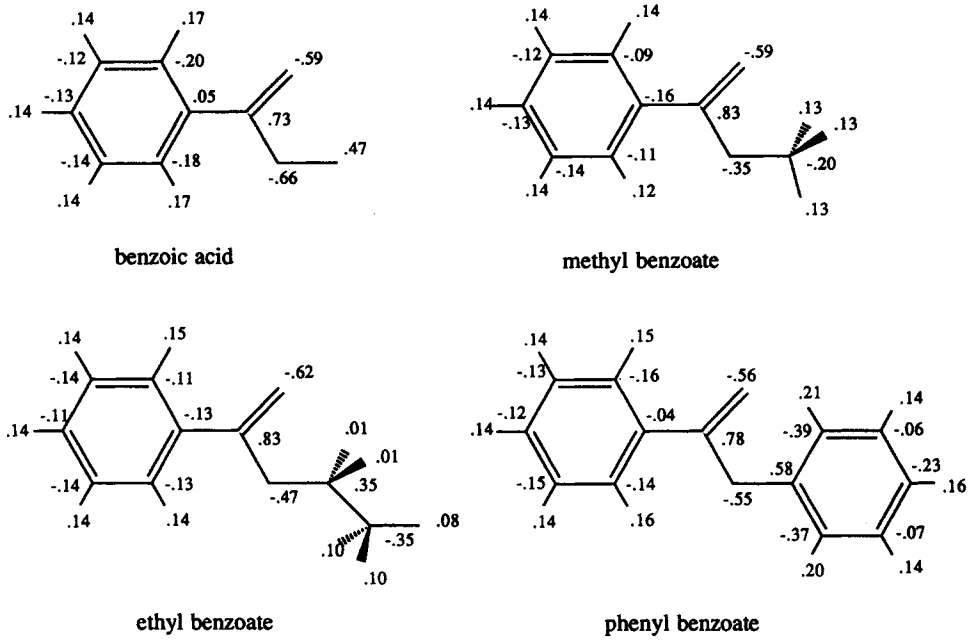

FIGURE 3. The ESP charges (in electron) of benzoic acid and its methyl, ethyl, and phenyl derivatives. These values were obtained by fitting the electrostatic potentials, which were calculated from HF/6-31G* wave functions, on the HF/6-31G* optimized structures. The standard RMS deviations of the least squares fits were less than 0.26 kcal/mol.

TABLE II.
Bond Increments Derived from the HF/6-31G* Electrostatic Potentials of Benzoic Acid (BA), Methyl Benzoate (MB), Ethyl Benzoate (EB), and Phenyl Benzoate (PB).

Bond	Atom types	BA	MB	EB	PB	Average	Final
C_1—O_2	c_1 o_1	0.59	0.59	0.62	0.56	0.59	0.531
C_1—C_3	c_1 cp	−0.05	0.08	0.04	0.02	0.02	0.018
C_1—O_4	c_1 0_2	0.19	0.16	0.17	0.24	0.18	0.171
H_{10}—O_4	h_1 o_2	0.47				0.47	0.423
C_{10}—O_4	c o_2		0.19	0.30		0.25	0.225
C_{10}—O_4	cp o_2				0.31	0.31	0.279

The final results given in the last column are used in the force field; they are obtained by multiplying the averaged values by a generic scaling factor of 0.9.

charge was assigned to the atom that is directly bonded to the ester group—C_3 or C_{10}. The following equations can be written according to eq. (5):

$$\left.\begin{aligned} Q_{C_1} &= \delta_{1,2} + \delta_{1,3} + \delta_{1,4} \\ Q_{O_2} &= -\delta_{1,2} \\ Q_{C_3} &= -\delta_{1,3} \\ Q_{O_4} &= -\delta_{1,4} \text{ ms } \delta_{4,10} \\ Q_{C_{10}} &= \delta_{4,10} \end{aligned}\right\} \quad (6)$$

Because the total charge must be zero, there are only four independent equations in eq. (6); hence these equations can be solved exactly for each of the molecules in Figure 3. The results are given in Table II. In the "averaged" column of Table II, the mean values of the calculated bond increments are listed. Finally, because the HF/6-31G* calculations overestimate systematically the experimental electrostatic properties, these averaged charges were scaled by a generic scaling factor of 0.9, which was obtained by a comparison of dipole moments between HF/6-31G* calculations and experimental data for a large group of organic compounds including ethers, esters, acids, alcohol, aldehydes, and ketones.[47] In the last column of Table II, the final results for the parameters used in the force field are listed.

The molecular dipole moments calculated for methyl, ethyl, and phenyl benzoates are given in Table III, with experimental data[60–63] for comparison. The HF/6-31G* values are those computed by the *ab initio* package TURBOMOLE, with the HF/6-31G* optimized structures. The ESP values were calculated by using the same optimized structures, but with ESP point charges as given in Figure 3. The force field results were calculated based on the force field optimized structures and the point charges derived from the bond increments given in the last column of Table II. It is apparent that the ESP charges can reproduce the HF/6-31G* dipole moments, which are systematically larger than the experimental values. The dipole moments calculated from the scaled charge parameters agree well with the experimental data. However, the overestimated partial charges with the HF/6-31G* calculations may be an appropriate choice for simulations for polarizable systems (e.g., water) in the condensed phase.[56]

The valence and cross-coupling parameters were derived by fitting to the quantum mechanical database with a nonlinear, least squares scheme, whereas the nonbonded parameters were fixed. The fit was generally satisfactory, with the values of RMS deviation of total energy less than 0.60 kcal/mol overall and a maximum deviation of total energy of 1.10 kcal/mol, for total energies ranging from 0 to over 100 kcal/mol. The parameters were then scaled by a standard set of scaling factors[1,5] that have been determined from comparisons between *ab initio* calculations and experimental data for a large number of organic molecules, including alkanes, acids, alcohols, aldehydes, ketones, amides, esters, etc.[1,5]

TABLE III.
Comparison of Dipole Moments of Methyl, Ethyl, and Phenyl Benzoate Molecules.

	Methyl	Ethyl	Phenyl
HF/6-31G*	2.086	2.185	2.022
ESP	2.083	2.193	2.049
Force field	1.881	1.903	1.814
Expt.[56–59]	1.84–1.94	2.00	1.80–1.92

Table IV lists the valence and cross-coupling parameters obtained here, with the exception of the parameters of alkyl and phenyl groups because they are given elsewhere.[5] All terms are given by the atom types which are defined in Table I. Examination of the bond and angle parameters reveals that they are anharmonic, as shown by large contributions from the cubic and quartic terms. Three sets of out-of-plane parameters are present; two of them are positive, consistent with the planarity of the carbonyl and the benzoyl groups. A negative value for the entry for (o_2 cp cp cp), which stands for the out-of-plane angle between the O_4—C_{10} bond and the C_{11}—C_{10}—C_{12} plane, results from the ester oxygen O_4 being slightly out of the phenyl ring plane in the optimized structure of phenyl benzoate. Torsional terms reflect the symmetry of the relevant rotations to an extend (e.g., a twofold function for rotation about a double or partial double bond, a three-fold function for rotation of a methyl group). Also, some of the torsion parameters are degenerated in a sense that the same parameters are used for several similar, but different, dihedral angles in which three of the four atoms types are the same. The cross-coupling terms are important for accurately accounting for vibrational frequencies and the changes of bond lengths and angles for different conformations. For example, it was found that frequency splitting of relevant vibrational modes is sensitive to the bond–bond, bond–angle coupling terms, and the bond–torsion coupling terms are important for conformational geometry changes.

Comparisons of the Molecular Mechanics Results of the Force Field with *Ab Initio* and Experimental Results

As a preliminary test of the force field developed, molecular mechanics calculations were conducted for methyl, ethyl, and phenyl benzoate and dimethyl terephthalate (DMT). The calculations were performed for conformations of rotations about three valence bonds: R, S, and T, as indicated in Figure 1, and defined by the dihedral angles C_5—C_3—C_1—O_4, C_3—C_1—O_4—C_{10}, and C_1—O_4—C_{10}—C_{11} of the model compounds, respectively (Fig. 2). The properties calculated are optimized structures and conformational energies and structures. In addition, vibrational frequencies were also calculated and compared with the experimental results for methyl benzoate.

METHYL BENZOATE

Three conformations of methyl benzoate were calculated, and the structural and energetic parameters are given in Table V with the results of *ab initio* HF/6-31G* calculations. The optimized structure was found to be a C_s symmetry species in which the phenyl group is coplanar with the ester (COO) group and the methyl group is trans to the phenyl group. The conformation with $\phi_R = 90°$ is a structure in which the phenyl ring is perpendicular to the ester plane. This structure is found to be the transition state of rotation of the phenyl ring, and the energy increment from the optimized structures is the rotation barrier height. The conformer with $\phi_S = 0°$ is a structure in which the methyl group is cis to the phenyl group.

Examination of the data given in Table V reveals that the structural parameters are sensitive to the conformation. Some of the bond lengths and angles are significantly different from one conformer to another. For example, the HF/6-31G* calculated bond lengths of the C_1—O_4 bond are 1.324 Å for the optimized, 1.323 Å for the $\phi_R = 90°$, and 1.331 Å for the $\phi_S = 0°$ structures; the respective angles of C_3—C_1—O_4 are 113.1°, 111.9°, and 118.2°. These changes of structural parameters show that the local environment can significantly influence the microscopic properties, as many other authors have pointed out.[6,64] The *ab initio* conformational structure changes have been reproduced qualitatively by the force field. For the same internals discussed earlier, the force field results are 1.366 Å, 1.362 Å, and 1.373 Å for the C_1—O_4 bond, and 112.0°, 110.0°, and 114.2° for the C_3—C_1—C_4 angle.

The conformational energies are also given in Table V. The barrier height of rotation about the *R* bond is 7.9 kcal/mol from HF/6-31G*, and 5.7 kcal/mol from the force field. The force field result agrees reasonably well with the experimental data of 5.3 kcal/mol, measured by an indirect infrared method[30] for methyl benzoate. The complete energy profile of rotation about the *R* bond was calculated using the force field, and the result is plotted in Figure 4. The calculations were performed by fixing the dihedral angle of C_5—C_3—C_1—O_4 at given values whereas all other degrees of freedom were relaxed. The curve shows that a single peak is located at a dihedral angle of 90°.

TABLE IV.
Valence and Cross-Coupling Parameters of the Force Field for Aromatic Polyesters.

Bond[a]	b_o (Å)	$k_2^{(b)}$	$k_3^{(b)}$	$k_4^{(b)}$
c_1 o_1	1.2020	851.1403	−1918.4882	2160.7659
c_1 o_2	1.3683	367.1481	−794.7908	1055.2319
c_1 cp	1.4890	339.3574	−655.7236	670.2362
o_2 h_1	0.9520	534.2994	−1287.1937	1889.1396
o_2 c	1.4457	326.7273	−608.5306	689.0333
o_2 cp	1.4098	387.9119	−715.9186	660.2442
Angle[a]	θ_o(°)	$k_2^{(a)}$	$k_3^{(a)}$	$k_4^{(a)}$
o_1 c_1 cp	125.5320	72.3167	−16.0650	2.0818
o_2 c_1 cp	108.4400	84.8377	−19.9640	2.7405
c_1 cp cp	116.0640	71.2598	−15.8273	2.0506
c_1 o_2 h_1	112.8740	53.2512	−14.9979	2.4640
c_1 o_2 c	113.2880	61.2868	−28.9786	7.9929
c_1 o_2 cp	113.0700	47.1131	−32.5592	13.1257
o_1 c_1 o_2	120.7970	95.3446	−32.2869	6.3778
o_2 c h	107.6880	65.4801	−10.3498	5.8866
o_2 c c	107.4100	63.3907	−13.4513	1.6650
o_2 cp cp	117.1400	33.0391	−14.7807	3.8573
cp cp cp	119.9000	61.0226	−34.9931	0.0000
Torsion[a]	$k_1^{(t)}$	$k_2^{(t)}$	$k_3^{(t)}$	
c_1 o_2 c c	0.0000	0.0000	−0.1932	
c_1 o_2 c h	0.0000	0.0000	−0.1932	
c_1 cp cp cp	0.0000	4.6282	0.0000	
o_2 cp cp cp	0.0000	2.5372	0.0000	
c_1 cp cp h	0.0000	2.1670	0.0000	
o_2 cp cp h	0.0000	2.1670	0.0000	
o_2 c c h	0.0000	0.0000	−0.2500	
o_2 c c c	0.0000	0.0000	−0.2500	
o_1 c_1 cp cp	0.0000	0.9063	0.0000	
o_2 c_1 cp cp	0.0000	0.9063	0.0000	
cp c_1 o_2 c	−1.1077	2.0082	0.0000	
cp c_1 o_2 cp	−1.1077	2.0082	0.0000	
cp c_1 o_2 h_1	−1.1077	2.0082	0.0000	
Out of plane[b]	$k_2^{(o)}$			
o_1 c_1 o_2 cp	49.3740			
c_1 cp cp cp	17.0526			
o_2 cp cp cp	−8.8126			
Bond, bond[c]	$k^{(bb')}$			
o_1 c_1 cp	116.9445			
o_2 c_1 cp	69.9445			
c_1 cp cp	37.8749			
c_1 o_2 c	45.4503			
c_1 o_2 cp	69.5999			
c_1 o_2 h_1	9.5671			
o_1 c_1 o_2	121.4880			
o_2 c c	23.2647			
o_2 c h	5.6454			
o_2 c o_2	8.2983			
o_2 cp cp	30.3889			

TABLE IV.
(Continued)

o_2 cp h	4.5800		
o_2 c_1 ny	84.5263		
Bond, angle[d]	$k^{(ba)}$	$k^{(b'a)}$	
o_1 c_1 cp	76.1093	72.8758	
o_2 c_1 cp	76.1093	72.8758	
c_1 cp cp	93.6977	45.8865	
c_1 cp cp	23.6977	45.8865	
o_2 cp cp	23.6766	49.6672	
c_1 o_2 c	46.4608	41.9116	
c_1 o_2 cp	64.3958	39.1599	
c_1 o_2 h_1	37.9163	21.4364	
o_1 c_1 o_2	76.2614	71.8761	
o_2 c c	47.9487	23.3920	
o_2 c h	57.4975	8.6864	
o_2 cz o_2	102.6457	102.6457	
o_2 cp cp	83.6766	49.6672	
Bond, torsion[e]	$k_1^{(bt)}$	$k_2^{(bt)}$	$k_3^{(bt)}$
c_1 o_2 c c	−5.4350	0.0000	0.0000
c_1 o_2 cp cp	0.0000	2.2650	0.0000
o_1 c_1 o_2 c	4.2600	0.0000	0.0000
o_1 c_1 o_2 cp	4.2600	0.0000	0.0000
o_1 c_1 o_2 h_1	4.2600	0.0000	0.0000
o_1 c_1 cp cp	0.0000	2.4002	0.0000
o_2 c_1 cp cp	0.0000	2.4002	0.0000
c_1 cp cp cp	0.0000	3.8762	0.0000

[a] The units for the nth force constants are kcal/mol/Å^n for bonds, kcal/mol/Rad^n for angles, and kcal/mol for torsions.
[b] The out-of-plane angle is defined by *ijkl*, where *j* is the center atom to which atoms *i*, *k*, and *l* are bonded.
[c] The bond–bond term of (*i*,*j*,*k*) is the coupling between bond *i*—*j* and *j*—*k*; atom *j* is the center one.
[d] Two bond–angle terms are given for (*i*,*j*,*k*), the angle is defined by *i*-*j*-*k*, two bonds are defined by *i*-*j*(*b*) and *j*-*k*(*b'*), respectively.
[e] The torsion angle is defined by *i*-*j*-*k*-*l*; the bond is defined by *j*-*k*.

TABLE V.
Comparison of Conformational Structures and Energies of Methyl Benzoate.

	HF/6-31G*			Force field		
	Opt	ϕ_R = 90°	ϕ_S = 0°	Opt	ϕ_R = 90°	ϕ_S = 0°
Bond (Å)						
C_3 C_1	1.490	1.501	1.507	1.489	1.509	1.508
C_1 O_2	1.191	1.188	1.183	1.204	1.200	1.200
C_1 O_4	1.324	1.323	1.331	1.366	1.362	1.373
O_4 C_{10}	1.416	1.418	1.413	1.443	1.443	1.438
Angle (°)						
C_5 C_3 C_1	122.1	120.0	120.1	122.5	120.2	120.6
C_6 C_3 C_1	118.0	120.0	119.9	119.1	120.2	119.9
C_3 C_1 O_2	124.0	124.6	122.1	126.4	127.0	125.3
C_3 C_1 O_4	113.1	111.9	118.2	112.0	110.0	114.2
C_1 O_4 C_{10}	116.9	116.9	122.7	117.8	117.6	123.1
Torsion (°)						
R (C_5 C_3 C_1 O_4)	180.0	90.0	93.1	180.0	90.0	102.6
S (C_3 C_1 O_4 C_{10})	180.0	180.0	0.0	180.0	180.0	0.0
δE (kcal/mol)	0.0	7.9	15.7	0.0	5.7	12.6

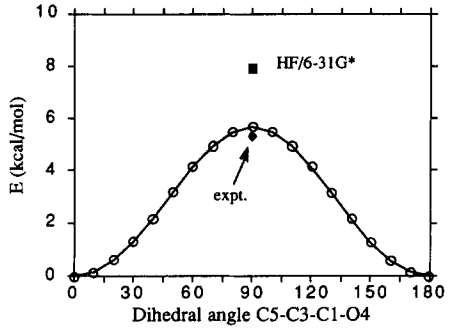

FIGURE 4. The force field optimized energy profile of rotation about the *R* bond in methyl benzoate. The HF/6-31G* and experimental energy barrier heights are labeled.

Rotation about the *S* bond is more restricted. The energy differences between the cis (ϕ_S = 0°) conformer and the optimized structure is 15.7 kcal/mol from the HF/6-31G* and 12.6 kcal/mol from the force field. Note that these values are much larger than the 5.1 kcal/mol calculated with the AM1 method.[34,35] However, this discrepancy falls in the same pattern found for the energies of rotation about the *R* bond, where the AM1 value is found to be 2.6 kcal/mol[31,34,35] and the HF/6-31G* result is 7.9 kcal/mol. Examination of the structural parameters given in Table V indicates the benzoyl group is not planar in the cis conformation; the C_5—C_3—C_1—O_4 dihedral angles are 93.1° from the HF/6-31G* and 102.6° from the force field, presumably due to the strong repulsion between the phenyl and the methyl groups. The structure is illustrated in Figure 5.

The force field energy profile of rotation about the *S* bond is plotted in Figure 6. It is interesting that ϕ_S = 0° is a transition state. In similar studies for carbonate[3] and urethane[65] molecules, the cis conformers were found to be local minimum energy structures, whereas transition states were found around ϕ_S = 80°. This, once again, reflects the effect of strong repulsion between the phenyl and methyl groups in the cis conformation of methyl benzoate.

ETHYL BENZOATE

Table VI lists structural and energetic parameters calculated for conformers of ethyl benzoate. Three conformations differing in rotations about the *T* bond (measured by the dihedral C_1—O_4—C_{10}—C_{11}) were calculated: an optimized anti structure, a gauche conformer at about ϕ_T = 80°, and a transition state at ϕ_T = 0°, in which the methyl group is cis to the carbonyl. Again, we see large deviations of some structural parameters among these conformers, and the force field can reproduce most of these changes qualitatively.

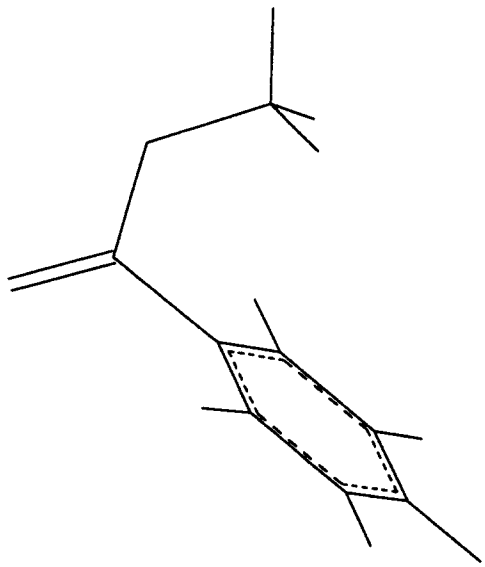

FIGURE 5. The optimized cis conformation of methyl benzoate.

The energy profile of rotation about the *T* bond is given in Figure 7. The second minimum, separated from the global minimum by a low-energy barrier, is located around ±80°. The energy increments from the global minimum to the second minimum are only 0.5 kcal/mol of the HF/6-31G* and 0.7 kcal/mol of the force field. This indicates that a distorted chain structure may well be found in the polyesters, as illustrated in Figure 8. The overall barrier heights of complete rotation were found to

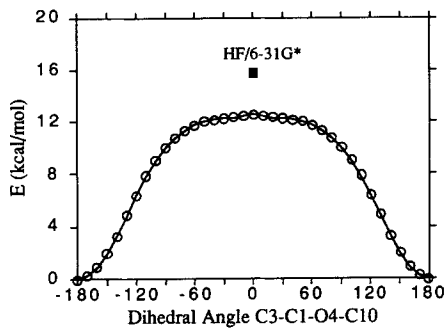

FIGURE 6. The force field optimized energy profile of rotation about the *S* bond in methyl benzoate. The HF/6-31G* energy barrier height is labeled.

TABLE VI.
Comparison of Conformational Structures and Energies of Ethyl Benzoate.

	HF/6-31G*			Force field		
	Anti	Gauche	Cis	Anti	Gauche	Cis
Bond (Å)						
C_3 C_1	1.491	1.491	1.495	1.489	1.490	1.495
C_1 O_2	1.192	1.192	1.191	1.204	1.204	1.202
C_1 O_4	1.323	1.323	1.320	1.363	1.364	1.356
O_4 C_{10}	1.424	1.426	1.432	1.436	1.446	1.449
C_{10} C_{11}	1.514	1.517	1.521	1.528	1.529	1.528
Angle (°)						
C_5 C_3 C_1	118.0	118.0	117.8	119.1	119.1	119.0
C_6 C_3 C_1	122.1	122.1	122.4	122.4	122.5	122.6
C_3 C_1 O_2	123.8	123.6	122.7	126.4	126.2	125.2
C_3 C_1 O_4	113.1	113.0	111.8	112.0	111.9	111.2
C_1 O_4 C_{10}	117.4	118.3	127.2	117.7	118.5	127.5
O_4 C_{10} C_{11}	107.4	111.5	119.5	107.6	108.6	115.9
Torsion (°)						
R (C_5 C_3 C_1 O_4)	180.0	179.9	180.0	180.0	179.6	180.0
S (C_3 C_1 O_4 C_{10})	180.0	179.8	180.0	180.0	176.7	180.0
T (C_1 O_4 C_{10} C_{11})	180.0	83.7	0.0	180.0	77.8	0.0
δE (kcal/mol)	0.0	0.5	7.9	0.0	0.7	7.8

be 7.9 kcal/mol from the HF/6-31G* and 7.8 kcal/mol from the force field. This energy barrier contains large contributions from the nonbonded interactions of the steric repulsion between the methyl and carbonyl group. One of the consequences of this steric repulsion is the large C_1—O_4—C_{10} angles of 127.2° from the HF/6-31G* and 127.5° from the force field. The small difference between the energy barriers of the HF/6-31G* and the force field is also due to the domination of nonbonded interactions—the scaling of valence parameters does not affect this barrier height significantly.

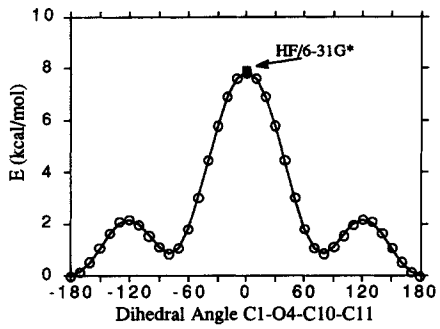

FIGURE 7. The force field optimized energy profile of rotation about the *T* bond in ethyl benzoate. The HF/6-31G* energy barrier height is labeled.

PHENYL BENZOATE

Table VII lists the structural and energetic parameters calculated for two conformations of phenyl benzoate, the optimized structure and a transition state (ϕ_T = 0°) of the rotation about *T* bond. The optimized structure belongs to C_1 symmetry, in which the benzoate group is planar, but the phenyl group attached to the ester oxygen is

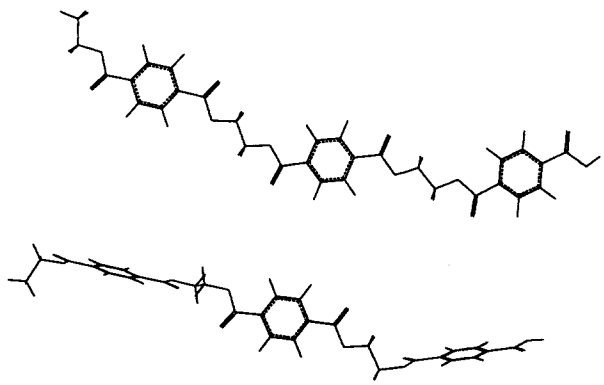

FIGURE 8. Comparison of two PET chain structures which contain anti and gauche ethylene groups, respectively. The gauche conformation is only 0.5–0.7 kcal/mol per bond higher in energy than the anti conformation, based on the HF/6-31G* and the force field calculations.

TABLE VII.
Comparison of Conformational Structures and Energies of Phenyl Benzoate.

	HF/6-31G*		Force field		
	Opt	ϕ_T = 0°	Opt	ϕ_T = 0°	Crystal
Bond (Å)					
C_3 C_1	1.489	1.491	1.491	1.494	1.48
C_1 O_2	1.186	1.188	1.204	1.203	1.20
C_1 O_4	1.340	1.331	1.356	1.345	1.36
O_4 C_{10}	1.383	1.380	1.400	1.389	1.41
Angle (°)					
C_5 C_3 C_1	117.7	117.6	119.1	119.1	118.1
C_6 C_3 C_1	122.3	122.6	122.4	122.5	122.5
C_3 C_1 O_2	124.5	123.5	126.1	125.6	126.2
C_3 C_1 O_4	112.2	111.7	111.9	111.7	111.7
C_1 O_4 C_{10}	119.3	127.0	118.7	126.7	118.8
O_4 C_{10} C_{11}	118.7	113.2	118.9	114.0	116.7
O_4 C_{10} C_{12}	119.7	126.0	122.3	128.6	120.6
Torsion (°)					
R (C_5 C_3 C_1 O_4)	179.8	180.0	179.3	180.0	173.8
S (C_3 C_1 O_4 C_{10})	179.5	180.0	179.2	180.0	180.0
T (C_1 O_4 C_{10} C_{11})	83.7	0.0	61.9	0.0	68.4
Out of plane (°)					
C_5 C_3 C_1 C_6	0.0	0.0	0.0	0.0	
O_4 C_{10} C_{11} C_{12}	3.0	0.0	5.6	0.0	
δE (kcal/mol)	0.0	1.4	0.0	1.5	

skewed. The ϕ_T = 0° conformation, which is planar, is a transition state of the rotation of the phenyl ring about the *T* bond. In Figure 9 the force field minimized energy profile of rotation of the phenyl ring about the *T* bond is given. In addition to the transition state of ϕ_T = 0°, there is another very low-energy transition state located at ϕ_T = 90°.

The HF/6-31G* result shows that the phenyl ring is in an almost perpendicular position with respect to the ester plane (ϕ_T = 83.7°) in the optimized

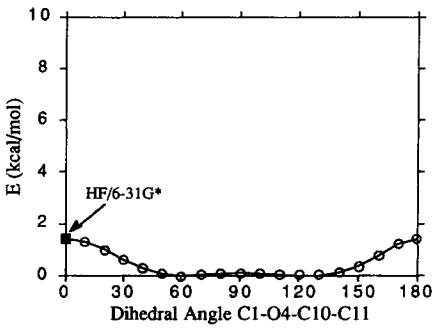

FIGURE 9. The force field optimized energy profile of rotation about the *T* bond in phenyl benzoate. The HF/6-31G* energy barrier height is labeled.

structure, whereas the force field result is 61.9° as illustrated in Figure 10. In our early calculations of phenyl carbonate[3] and phenyl carbamate,[65] it was found that this angle is about 65° at the same HF/6-31G* level of theory. This discrepancy indicates that the interaction between the two phenyl rings, which are separated by the COO group in phenyl benzoate, is strong enough to overcome the very low-energy barrier (0.01–0.04 kcal/mol at ϕ_T = 90° for phenyl carbonate and phenyl carbamate). However, calculations on phenyl carbamate reveal that the torsion angle changes from 65.6 to 59.1 (ref. 65) when the electron correlation is corrected by Møller–Plesset second-order perturbation theory (MP2)[66] with the 6-31G* basis set. Along with the shift of the torsional angle, the barrier heights increase from 0.04 to 0.43 kcal/mol at ϕ_T = 90°; and from 1.10 to 1.38 kcal/mol at ϕ_T = 0°.[65] Based on these results, one may expect that at the MP2/6-31G* level, the torsion angle of C_1—O_4—C_{10}—C_{11} in phenyl benzoate should be smaller than 83°. The actual calculation was too expensive to be carried out in this study.

In Table VII, the "idealized" crystal structure values[35] for benzoate functional groups, which are mean values of 10 benzoate crystals after excluding

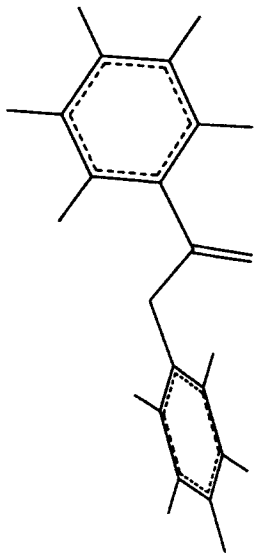

FIGURE 10. Illustration of the optimized structure of phenyl benzoate.

unexpectedly deviant values,[35] are included for comparison. It is important to point out that the comparison of the calculated results for the isolated molecules with those measured in condensed phases is not strictly valid because the local environment may have a significant impact on the measured structural parameters. This is evident partly by the fact that measured crystal structures exhibit large deviations for the same internals in different crystals.[35] Nevertheless, the comparison shows reasonably good agreement between the force field optimized structure and the crystal data for bond lengths and most bond angles.

DIMETHYL TEREPHTHALATE

The minimized structure of DMT is planar with both ester groups coplanar with the phenylene group. Therefore, the ester groups of DMT may be either trans (as shown in Fig. 2) or cis with respect to each other. The energy difference between these two conformers has been studied. Based on dipole moment analysis, Saiz, Hummel, Flory, and Plavsic deduced that the electrostatic energy of the cis conformer exceeds that of the trans by approximately 0.050 kcal/mol.[60] Lautenschlager et al.[36] reported their calculation results of terephthalic acid from which the energy differences between these two conformations are 0.0 kcal/mol from both AM1 and CVFF force field calculations, more than 2.5 kcal/mol from the *ab initio* HF/STO-3G and HF/3-21G calculations. The substantial discrepancies between their *ab initio* results and the experimental data were not explained.[36]

The trans and cis conformations of terephthalic acid were calculated in this study by fully optimizing these conformations at HF/3-21G and HF/6-31G* levels of theory. The trans conformation was found to be more stable than the cis, and the energy differences between these two conformations are 0.041 kcal/mol with HF/3-21G and 0.051 kcal/mol with HF/6-31G*.

The optimizations were also performed on trans and cis conformations of DMT by using the force field, which led to an energy difference of 0.062 kcal/mol between these two conformations. Analysis of the energy partitions shows that the total 0.062 kcal/mol difference between the trans and cis conformers is mostly from the Coulomb interaction. In fact, the value of 0.055 kcal/mol for the Coulomb contribution (basically a dipole–dipole interaction) agrees extremely well with that estimated by Saiz, Hummel, Flory, and Plavsic.[60] Furthermore, the energy analysis suggests that the total energy is slightly larger than the electrostatic energy. This information is extremely difficult to obtain from experiments but is a straightforward task for force field methods.

VIBRATIONAL FREQUENCIES

Finally, normal mode vibrational frequencies were calculated for methyl benzoate, for which the experimental spectrum has been resolved.[67] The calculations were conducted with HF/6-31G* and the force field. The assignments of the calculated normal modes to internal coordinates were conducted by using a simple scheme based on the B-matrix method.[68] The results are listed in Table VIII, with experimental data[67] for comparison.

This is another example with which to illustrate the validity of using the scaling factors to scale the *ab initio* force field parameters. Comparison of the frequencies given in the table shows that the HF/6-31G* frequencies are generally overestimated, but the force field results agree reasonably well with the experimental data. This difference indicates the effect of scaling factors, which systematically scaled down the force constants, and hence the vibrational frequencies.

Conclusions

Based on *ab initio* HF/6-31G* calculations and known experimental data, an all-atom CFF93 type

TABLE VIII.
Comparison of Vibrational Frequencies (in cm^{-1}) of Methyl Benzoate.

No.	HF/6-31G*	Force field	IR	Raman	Approx. assignment
1	3415	3090		3075	Phenyl C—H stretching
2	3411	3082			Phenyl C—H stretching
3	3387	3079			Phenyl C—H stretching
4	3375	3076			Phenyl C—H stretching
5	3360	3062			Phenyl C—H stretching
6	3348	2973		2951	Methyl C—H stretching
7	3334	2969		2951	Methyl C—H stretching
8	3251	2891		2851	Methyl C—H stretching
9	1992	1727	1722	1722	C=O stretching
10	1811	1615	1600	1605	Phenyl
11	1787	1547	1578	1582	Phenyl
12	1672	1474	1492	1495	Phenyl
13	1650	1490			Methyl bending
15	1643	1487	1434	1438	Methyl bending
16	1633	1479	1434	1438	Methyl bending
14	1616	1432	1451	1455	Phenyl
17	1473	1325	1313	1317	Phenyl
18	1352	1284	1275	1280	Phenyl
19	1455	1258	1258	1258	Skeletal stretching
20	1347	1188	1190	1193	Methyl deformation
23	1298	1162	1158	1161	Methyl deformation
21	1299	1161	1174	1178	Phenyl
22	1232	1154	1158	1161	Phenyl
24	1256	1116	1114	1112	Skeletal stretching
25	1183	1056	1068	1074	Phenyl
26	1136	993	1024	1028	Phenyl out_p
27	1131	990	1000	1004	Phenyl out_p
28	1117	989			Phenyl out_p
29	1095	963		970	Phenyl wag
30	1089	960	963	968	Skeletal stretching
31	1077	915	934		Phenyl wag
32	964	882	850	851	Phenyl wag
33	914	775	818	818	Skeletal bending
34	908	852	802	808	Phenyl output
35	805	750	710		Phenyl output
36	758	681	685		Phenyl torsion
37	741	675	672	676	Phenyl input deformation
38	676	628	612	620	Phenyl input deformation
39	494	485			Phenyl torsion
40	520	482	485	482	Skeletal bending
41	456	420		410	Phenyl torsion
42	384	360	358	360	Skeletal bending
43	354	353		332	Skeletal bending
44	221	217		218	Methyl torsion
45	177	188			Skeletal bending
46	176	187			Methyl torsion
47	117	108			Skeletal torsion
48	62	52			Skeletal torsion

force field has been developed for aromatic polyesters.

The nonbonded van der Waals parameters were transferred from similar molecular systems from which the nonbonded parameters were derived by fitting to the crystal structures. The atomic partial charges were derived by fitting to the *ab initio* electrostatic potentials (ESP) calculated for a group of model compounds, at the HF/6-31G* level of theory. The valence parameters were obtained by fitting to the total energies, first and second derivatives of the total energies of the model molecules, which were distorted along their normal mode coordinates to sample the intramolecular interactions. The valence, cross-coupling, and charge parameters were then scaled by a set of generic parameters to correct for the systematic errors of HF/6-31G* calculations.

By including all degrees of freedom and rather complex functional forms, the developed force field is more flexible than those previously proposed for aromatic esters. Specifically, large changes in valence coordinates found to accompany conformational changes have been reproduced qualitatively by the force field calculations. The calculated vibrational frequencies agree well with the experimental results.

Molecular mechanics calculations using the proposed force field provide detailed information of the conformational energies, structures, and dipole moments for aromatic ester functional groups. The energy barrier height for rotation about the C(phenyl)—C(carbonyl) bond is found to be 5.7 kcal/mol, which agrees well with the experimental value of 5.3 kcal/mol. The rotation about C(carbonyl)—O(ester) is more restricted, with an energy barrier height of more than 12 kcal/mol. The rotation about O(ester)—C(alkyl) and O(ester)—C(phenyl) bonds is much less restricted; in the former case, a second minimum on the energy profile indicates that a gauche conformation is only a fraction of a kcal/mol per bond less stable than the anti conformation. The *ab initio* and force field calculations on trans and cis conformations of terephthalic acid and dimethyl terephthalate (DMT) show that the energy differences between the two conformations are in a range of 0.041 and 0.062 kcal/mol. An energy analysis of the force field results shows that 0.055 kcal/mol of the total energy difference of 0.062 kcal/mol is due to the electrostatic dipole–dipole interaction, which agrees extremely well with the experimental data.

Acknowledgment

This work was supported as part of Biosym Technologies' Polymer Project, which was funded by a consortium of 50 companies and government laboratories. The author thanks Dr. A. T. Hagler for many beneficial discussions about force field development and Dr. B. E. Eichinger and Dr. S. J. Mumby for reviewing the manuscript.

References

1. J. A. Maple, M. J. Hwang, T. P. Stockfisch, U. Dinur, M. Waldman, C. S. Ewig, and A. T. Hagler, *J. Comp. Chem.*, in press.
2. U. W. Suter, *Makromolekulare Chemie-Macromolecular Symposia*, **65**, 1 (1993).
3. K. Kremer, B. Dunweg, and M. S. Stevens, *Physica A*, **194**, 321 (1993).
4. K. Binder, *Makromolekulare Chemie-Macromolecular Symposia*, **69**, 213 (1993).
5. M. J. Hwang, T. P. Stockfisch, and A. T. Hagler, *J. Am. Chem. Soc.*, to be published.
6. H. Sun, S. J. Mumby, J. R. Maple, and A. T. Hagler, *J. Am. Chem. Soc.*, to be published.
7. (a) A. T. Hagler, E. Huler, and S. Lifson, *J. Am. Chem. Soc.*, **96**, 5319 (1974); (b) A. T. Hagler and S. Lifson, *J. Am. Chem. Soc.*, **96**, 5327 (1974).
8. (a) F. A. Momany, R. F. McGuire, A. W. Burgess, and H. A. Scheraga, *J. Phys. Chem.*, **79**, 2361 (1975); (b) F. A. Momany, L. M. Carruthers, R. F. McGuire, and H. A. Scheraga, *J. Phys. Chem.*, **78**, 1595 (1974); (c) F. A. Momany, L. M. Carruthers, and H. A. Scheraga, *J. Phys. Chem.*, **78**, 1621 (1974).
9. U. Burkert and N. L. Allinger, *Molecular Mechanics*, American Chemical Society, Washington, DC, 1982.
10. (a) S. J. Weiner, P. A. Kollman, D. A. Case, U. C. Singh, C. Ghio, G. Alagona, S. Profeta, and P. Weiner, *J. Am. Chem. Soc.*, **106**, 765 (1984); (b) S. J. Weiner, P. A. Kollman, D. T. Nguyen, and D. A. Case, *J. Comp. Chem.*, **7**, 230 (1986).
11. P. Dauber-Osguthorpe, V. A. Roberts, D. J. Osguthorpe, J. Wolff, M. Genest, and A. T. Hagler, *Proteins: Struct., Func., Gen.*, **4**, 31 (1988).
12. B. R. Gelin and M. Karplus, *Biochemistry*, **18**, 1256 (1979).
13. B. D. Olafson, D. J. States, S. Swaminathan, and M. Karplus, *J. Comp. Chem.*, **4**, 187 (1983).
14. L. Nilsson and M. Karplus, *J. Comp. Chem.*, **7**, 591 (1986).
15. N. L. Allinger, Y. H. Yuh, and J. H. Lii, *J. Am. Chem. Soc.*, **111**, 8551 (1989).
16. (a) J. H. Lii and N. L. Allinger, *J. Am. Chem. Soc.*, **111**, 8566 (1989); (b) J. H. Lii and N. L. Allinger, *J. Am. Chem. Soc.*, **111**, 8567 (1989); (c) J. H. Lii and N. L. Allinger, *J. Comp. Chem.*, **12**, 186 (1991).
17. N. L. Allinger, F. B. Li, L. Q. Yan, and J. C. Tai, *J. Comp. Chem.*, **11**, 868 (1990).

18. S. Dasgupta and W. A. Goddard, *J. Chem. Phys.*, **90,** 7207 (1989).
19. S. L. Mayo, B. D. Olafson, and W. A. Goddard, *J. Phys. Chem.*, **94,** 8897 (1990).
20. A. K. Rappé, C. J. Casewit, K. S. Colwell, W. A. Goddard, and W. M. Skiff, *J. Am. Chem. Soc.*, **114,** 10024 (1992).
21. T. Halgren, *J. Am. Chem. Soc.*, **112,** 4710 (1990).
22. P. Amodeo and V. Barone, *J. Am. Chem. Soc.*, **114,** 9085 (1992).
23. W. J. Hehre, L. Radom, and J. A. Pople, *J. Am. Chem. Soc.*, **94,** 1496 (1972).
24. W. J. Hehre, R. F. Stewart, and J. A. Pople, *J. Chem. Phys.*, **51,** 2657 (1969).
25. T. Schaeffer, T. A. Wildman, and R. Sebastian, *J. Mol. Structr. Theochem.*, **89,** 93 (1982).
26. T. Schaeffer, G. H. Penner, *Can. J. Chem.*, **65,** 2175 (1987).
27. J. S. Binkley, J. A. Pople, and W. H. Hehre, *J. Am. Chem. Soc.*, **102,** 939 (1980).
28. P. Pulay, G. Fogarasi, F. Pang, and J. E. Boggs, *J. Am. Chem. Soc.*, **101,** 2550 (1979).
29. S. Marriott and R. D. Topsom, *Aust. J. Chem.*, **39,** 1157 (1986).
30. T. B. Grindley, A. R. Katritzky, and R. D. Topsom, *J. Chem. Soc., Perkin Trans.*, 274, 289 (1974).
31. B. Coussens, K. Pierloot, and R. J. Meier, *J. Mol. Structr. Theochem.*, **259,** 331 (1992).
32. W. J. Hehre, L. Radom, P. R. Schleyer, and J. A. Pople, *Ab Initio Molecular Orbital Theory*, John Wiley & Sons, New York, 1986.
33. N. L. Allinger, R. S. Grev, B. F. Yates, and H. F. Schaefer, *J. Am. Chem. Soc.*, **112,** 114 (1990).
34. M. Fabian, *J. Comp. Chem.*, **9,** 369 (1988).
35. P. Coulter and A. H. Windle, *Macromolecules*, **22,** 1129 (1989).
36. P. Lautenschlager, J. Brickmann, J. Ruiten, and R. J. Meier, *Macromolecules*, **24,** 1284 (1991).
37. R. K. Kakar, E. A. Rinehart, C. R. Quade, and T. Kojima, *J. Chem. Phys.*, **52,** 3803 (1970).
38. J. R. Durig, H. D. Bist, K. Furic, J. Qiu, and T. S. Little, *J. Mol. Structr.*, **129,** 45 (1985).
39. J. P. Hummel and P. J. Flory, *Macromolecules*, **13,** 479 (1980).
40. T. L. Hill, *J. Chem. Phys.*, **16,** 399 (1948).
41. N. L. Allinger and S. H. Chang, *Tetrahedron*, **33,** 1561 (1977).
42. (a) M. Haeser and R. Ahlrichs, *J. Comp. Chem.*, **10,** 104 (1989); (b) R. Ahlrichs, M. Baer, M. Haeser, H. Horn, C. Koelmel, *Chem. Phys. Lett.*, **162,** 165 (1989).
43. GAUSSIAN90, Gaussian, Inc., Pittsburgh, PA, 1990.
44. PROBE-V1.1, DISCOVER-V2.9, Biosym Tech. Inc., San Diego, CA, 1992.
45. (a) W. H. Hehre, R. Ditchfield, and J. A. Pople, *J. Chem. Phys.*, **56,** 2257 (1972); P. C. Hariharam and J. A. Pople, *Theor. Chim. Acta.*, **28,** 213 (1973).
46. A. T. Hagler, S. Lifson, and P. Dauber, *J. Am. Chem. Soc.*, **101,** 5122 (1979).
47. H. Sun, unpublished results.
48. R. S. Mulliken, *J. Chem. Phys.*, **23,** 1833 (1955).
49. E. R. Davidson, *J. Chem. Phys.*, **46,** 3320 (1967).
50. U. Dinur and A. T. Hagler, *J. Chem. Phys.*, **91,** 2949 (1989).
51. (a) D. E. Williams and J.-M. Yan, *Adv. Atom. Mol. Physics*, **23,** 87 (1988); (b) D. E. Williams, *J. Comp. Chem.*, **9,** 745 (1988); (c) D. E. Williams, *Biopolymers*, **29,** 1367 (1990).
52. F. Colonna, J. G. Ángyán, and O. Tapia, *Chem. Phys. Lett.*, **172,** 55 (1990).
53. C. M. Breneman and K. B. Wiberg, *J. Comp. Chem.*, **3,** 361 (1990).
54. F. Colonna, E. Evlethand, and J. G. Ángyán, *J. Comp. Chem.*, **13,** 1234 (1992).
55. H. J. Urban and G. R. Famini, *J. Comp. Chem.*, **14,** 353 (1993).
56. (a) O. Cieplak and P. Kollman, *J. Comp. Chem.*, **12,** 1232 (1991); (b) P. D. J. Grootenhuis and P. Kollman, *J. Am. Chem. Soc.*, **110,** 1657 (1988); (c) S. Rao and P. Kollman, *Biopolymers*, **25,** 267 (1986).
57. A. T. Hagler and A. Lapicirella, In *Peptides: Chemistry, Structure and Biology*, R. Walter and J. Meienhofer, Eds., Ann Arbor Science Publishers, Ann Arbor, MI, 1975, p. 279.
58. F. L. Hirschfeld, *Theor. Chim. Acta.*, **44,** 129 (1977).
59. P. Coppens and E. D. Stevens, *Adv. Quant. Chem.*, **10,** 1 (1977).
60. E. Saiz, J. P. Hummel, P. J. Flory, and J. Plavsic, *J. Phys. Chem.*, **85,** 3211 (1981).
61. R. D. Nelson, D. R. Lide, and A. A. Maryott, *Selected Values of Electric Dipole Moments for Molecules in the Gas Phase*, National Standards Reference Data Series, National Bureau of Standards, Washington, U.S. Government Printing Office, 1967.
62. A. L. McClellan, *Tables of Experimental Dipole Moments*, Vol. II, Rahara Enterprises, El Cerrito, CA, 1974.
63. BEILSTEIN database, Springer-Verlag, New York, 1993.
64. L. Schafer, S. Q. Newton, F. A. Momany, and V. J. Llimkowski, *J. Mol. Structr. Theo.*, **78,** 275 (1991).
65. H. Sun, *Macromolecules*, **26,** 5924 (1993).
66. (a) J. A. Pople, R. Seeger, and R. Krishnan, *Int. Quantum Chem.*, **11S,** 149 (1977); (b) R. Krishnan and J. A. Pople, *Int. Quantum Chem.*, **14,** 91 (1978).
67. F. J. Boerio and S. K. Bahl, *Spectr. Acta*, **32A,** 987 (1976).
68. E. B. Wilson, J. C. Decius, and P. C. Cross, *Molecular Vibrations*, McGraw-Hill, New York, 1955.